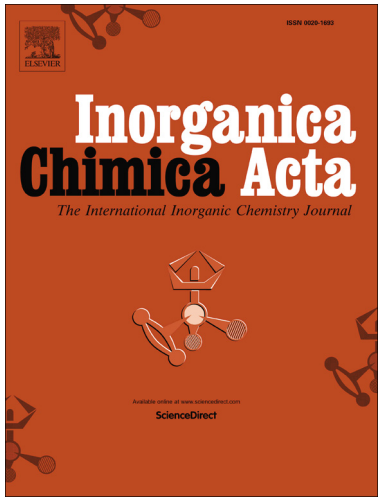

Research paper

Zn Thiosacharinates: from ionic to polymeric structures. Synthesis, characterization and cell proliferation inhibition studies

Fermín Delgado, Eleonora Freire, Ricardo Baggio, Verónica González Pardo, Viviana Dorn, Mariana Dennehy

PII: S0020-1693(18)30289-5
DOI: https://doi.org/10.1016/j.ica.2018.04.040
Reference: ICA 18231

To appear in: *Inorganica Chimica Acta*

Received Date: 20 February 2018
Revised Date: 19 April 2018
Accepted Date: 20 April 2018

Please cite this article as: F. Delgado, E. Freire, R. Baggio, V.G. Pardo, V. Dorn, M. Dennehy, Zn Thiosacharinates: from ionic to polymeric structures. Synthesis, characterization and cell proliferation inhibition studies, *Inorganica Chimica Acta* (2018), doi: https://doi.org/10.1016/j.ica.2018.04.040

Zn Thiosacharinates: from ionic to polymeric structures.

Synthesis, characterization and cell proliferation inhibition studies

Fermín Delgado[a], Eleonora Freire[b,c], Ricardo Baggio[b], Verónica González Pardo[d], Viviana Dorn[a], Mariana Dennehy[a*]

[a] INQUISUR/ Departamento de Química, Universidad Nacional del Sur, Bahía Blanca, Argentina
[b] Gerencia de Investigación y Aplicaciones, Centro Atómico Constituyentes, Comisión Nacional de Energía Atómica, Buenos Aires, Argentina
[c] Escuela de Ciencia y Tecnología, Universidad Nacional General San Martín, Buenos Aires, Argentina.
[d] INBIOSUR/Departamento de Biología, Bioquímica y Farmacia, Universidad Nacional del Sur, Bahía Blanca, Argentina

*Correspondence e-mail: mdennehy@uns.edu.ar

Abstract

A series of Zn thiosacharinates complexes with nitrogen donor co-ligands were synthesized: $[Zn(tsac)_2(o\text{-}phen)]$, $[Zn(tsac)_2(TMDP)]_n$, $[(4,4'\text{-}bipy)H_2][Zn(tsac)_4]$ $[Zn(tsac)_2(2,2'\text{-}bipy)]$, $[Zn(tsac)_2(2,2'\text{-}bquin)]$, (tsac, thiosaccharinate anion: 1,1-dioxo-1,2-benzisothiazole-3-thiolato, $C_7H_4NO_2S_2^-$, o-phen: 1,10'-phenantroline, TMDP: trimethylenedipyridine, 2,2'-bipy: 2,2'-bipyridine, 4,4'-bipy: 4,4'-bipyridine, 2,2'-bquin: 2,2'-biquinoline). They were fully characterized by means of FTIR, ^{13}C and ^{1}H NMR, elemental analysis and conductivity measurements. Three of them, $[Zn(tsac)_2(o\text{-}phen)]$, $[(4,4'\text{-}bipy)H_2][Zn(tsac)_4]$, $[Zn(tsac)_2(TMDP)]_n$ were also characterized by X-ray single crystal diffractometry and their crystal structures are described herein. DFT geometry optimization for the $[Zn(tsac)_2(o\text{-}phen)]$ complex was performed and its vibrational spectra was predicted. Moreover, we studied the effects of the five complexes on cell proliferation, thus providing preliminary evidence for their therapeutic potential as anti-cancer drugs.

Keywords: Zinc, thionate, biological activity, crystal structure, nitrogenated ligands, cell proliferation inhibition

Introduction

Zn shows an indispensable role and it is considered as a fundamental trace element for living organisms. An increased amount in the published research shows the importance of this metal complexes and refutes its "boring element" tag. It acts as a divalent cation when it binds to enzymes and other proteins on its biochemical functions. Moreover, coordination complexes with the presence of Zinc (II) ion are essential in the function of several bio-molecules. It acts as the active site of enzymes (it is vital for the functionality of more than 300 enzymes) [1,2]. Diverse metabolic paths that are dependent on this metal have been recognized and studied so far. Additionally, several Zinc based compounds have been used as antifungal and antibacterial [3,4]. On the other hand, the coordination chemistry of different types of poly-dentate organic nitrogen–sulfur ligands is an interesting and developing field of research and has generated

considerable recent interest [5,6]. Complexes of these systems are involved in the catalysis of different biological processes and thus, they receive attention nowadays. For all these reasons, sulfur-rich zinc sites in metallo-proteins could be better understood with the synthesis and characterization of ternary Zinc-thionate complexes. Among the different possible co-ligands, bi-pyridyl ligands are good building blocks that allow the construction of a variety of complexes with defined geometry and symmetry and could enable the formation of strong complexes. These type of N,N-bidentate ligands are also of importance due to their possible activity against different types of bacteria.

Because of the bulky S atom with the vicinity of the amide N atom, considerable bridging capabilities are found for heterocyclic thionates, the deprotonated form of thiones. As other heterocyclic chalcogenones, thiosaccharine (the thione form of saccharin, $C_6H_4S(O)_2NHC(S)$, 1,1-dioxo-1,2-benzisothiazole-3-thione) can bind a metal ion in its anionic form either as monodentate species either via the thionate sulphur atom or the thioamido nitrogen atom, or as an ambidentate ligand via a variety of bonding modes. The coordination chemistry of thiosaccharine with several transition metals (Cd, Tl, Pd, Pt, Ag, Au, Cu, Bi) has been previously investigated and reported in detail [7,8,9 and references therein]. So far, the versatility of this anion has been extensively demonstrated in the different complexes described. At this point, surprisingly, the coordination of Zn to this thionate remains unexplored.

For this reason, in the present work, we report the synthesis and full characterization of a series of Zn thiosaccharinates with N ancillary aromatic co-ligands, $[Zn(tsac)_2(o\text{-phen})]$ (**1**), $[Zn(tsac)_2(TMDP)]_n$ (**2**), $[(4,4'\text{-bipy})H_2][Zn(tsac)_4]$ (**3**), $[Zn(tsac)_2(2,2'\text{-bipy})]$ (**4**) and $[Zn(tsac)_2(2,2'\text{-bquin})]$ (**5**). Moreover, we inform here their effects on cell proliferation inhibition, thus providing preliminary evidence for their therapeutic potential as anti-cancer drugs.

2. Experimental

2.1. General remarks

All reagents were of commercial analytical quality and used without further purification. The solid thiosaccharin (Hthiosaccharinate) in its α-form was synthesized when Lawesson's reagent (3.64 g; Fluka) reacted with acid saccharin (3.00 g; Mallinckrodt) in toluene solution (25 mL), following the technique published by Schibye *et al.* [10]. The FTIR spectra of the substances as KBr dispersions were registered in the 4000–400 cm^{-1} range on a Thermo Scientific Nicolet iS50 FTIR-NIR spectrometer. Nuclear magnetic resonance (NMR) spectra were recorded on a Bruker ARX-300 spectrophotometer using the residual solvent peak as an internal reference. The NMR studies were performed in deuterated dimethylsulfoxide, DMSO-d^6 solutions. The C, H, and N elemental analyses were performed with a CE440 Elemental Analyzer. and were found to be in good agreement with the calculated values. Conductivity measurements were performed with a digital OAKTON conductimeter, which was calibrated with a KCl aqueous solution (744.7 ppm, 1413 µS). The conductivity measurements were performed in DMSO.

2.2 Synthesis of the complexes

$[Zn(tsac)_2(o\text{-phen})]$ (1)

The $[Zn(tsac)_2(o\text{-phen})]$ complex was prepared by addition of a dissolution of $Zn(NO_3)_2{\cdot}6H_2O$ (14.85 mg, 0.049 mmol, 2 mL) into a thiosaccharine solution (20 mg, 0.1 mmol/ ethanol:water 1:1, 2 mL). A o-phenantroline solution was finally added drop by drop (ethanol:water 1:1, 2 mL) and a yellow power was obtained. The resulting yellow solid was filtered and washed

with cold water. Crystals suitable for X-ray diffraction studies were produced by slow diffusion of diethyl ether to the mother solution. Yield: 74 % Molar Conductivity ($\mu S\ M^{-1}$) = 22.4. Calculated analytical percent composition for $C_{26}H_{16}N_4O_4S_4Zn$: C=48.516%; H=2.267%; N=8.592%; Found: C= 48.638%; H=2.511%; N=8.725%. Soluble in dimethyl sulfoxide and dimethyl formamide. Non-soluble in other solvents (methanol, chloroform, dichloromethane, acetone, water). UV-Visible [DMSO, λmax nm]: 341

^{1}H NMR (300 MHz, DMSO) δ 8.72-9.21 (m, 1H), 8.94 (m, 1H), 8.31 (m, 1H), 8.03-8.21 (m, 1H), 7.91 (m, 1H), 7.57-7.72 (m, 3H). ^{13}C NMR (75 MHz, DMSO) δ 191.81 (C1), 149.09 (C8), 140.02 (C10), 139.36 (C12), 137.94 (C7), 136.52 (C2), 132.12 (C4), 130.91 (C5), 128.70 (C11), 127.37 (C13), 125.10 (C3), 125.81 (C9), 119.03 (C6).

$[Zn(tsac)_2(TMDP)]_n$ (2)

The complex was synthesized by addition of 4,4′-trimethylenedipyridine (6.2 mg, 0.031 mmol) and thiosaccharine (12.7 mg, 0.0638 mmol), respectively, to a solution of $Zn(NO_3)_2{\cdot}6H_2O$ (10.2 mg, 0.0342 mmol) in ethanol:water (4 ml), and kept under mechanical stirring at room temperature. The resulting yellow solid was filtered off and washed with cold water. By slow evaporation of the mother solution single crystals appeared. They were washed with water and analysed using X-ray diffraction. Yield: 82%. Molar conductivity ($\mu S\ M^{-1}$) = 28.3. Analytical percent composition calculated for $C_{27}H_{22}N_4O_4S_4Zn$: C=49.127%; H=3.359%; N=8.487%. Found:C=48.811%; H=2.981%; N=8.378%.

Soluble in DMSO and DMF. Slightly soluble in water, ethanol, methanol, chloroform. Insoluble in acetone and methane dichloride. UV-Visible [DMSO, λmax nm]: 347

^{1}H NMR (300 MHz, DMSO) δ 8.46 (dd, 4H), 7.92 (m, 2H), 7.58-7.72 (m, 6H), 7.28 (dd, 4H), 2.64 (t, 4H), 1.93 (m, 2H). ^{13}C NMR (75 MHz, DMSO) δ 191.71 (C1), 151.07 (C10), 149.31 (C8), 137.98 (C7), 136.56 (C2), 132.05 (C4), 130.82 (C5), 125.07 (C3), 124.04 (C9), 119.01 (C6), 33.80 (C11), 30.12 (C12).

$[(4,4'\text{-bipy})H_2][Zn(tsac)_4]$ (3)

It was obtained by addition of 4,4'-bipyridine (7.7 mg, 0.049 mmol) and thiosaccharine (20.3 mg, 0.102 mmol), to a dissolution of $Zn(NO_3)_2{\cdot}6H_2O$ (15.2 mg, 0.0511 mmol) in water/ethanol 1:1, with mechanical stirring at ambient temperature. The resulting yellow precipitate was washed with water and dried. Yellow crystals, suitable for X-ray diffraction studies were obtained. Yield: 26.9%. Molar Conductivity ($\mu S\ M^{-1}$) = 138.7.

Analytical percent composition calculated for $C_{38}H_{26}N_6O_8S_8Zn$: C=44.901%; H=2.580%; N=8.270%. Found: C=45.996%; H=2.473%; N=8.446%.

Soluble in dimethyl sulfoxide and dimethyl formamide. Slightly soluble in water, ethanol, methanol and chloroform. Insoluble in acetone and dichloromethane. UV-Visible [DMSO, λmax nm]: 340

^{1}H NMR (300 MHz, DMSO) δ 8.98 (dd, 4H), 8.30 (dd, 4H), 7.87-8.02 (m, 4H), 7.73-7.81 (m, 4H), 7.35-7.72 (m, 10H). ^{13}C NMR (75 MHz, DMSO) δ 191.56 (C1), 148.94 (C8), 145.88 (C10), 137.88 (C7), 136.35 (C2), 132.28 (C4), 131.11 (C5), 125.16 (C3), 122.38 (C9), 119.15 (C6).

$[Zn(tsac)_2(2,2'\text{-bipy})]$ (4)

This complex was prepared in a similar way as (**1**): $Zn(NO_3)_2{\cdot}6\ H_2O$ (11 mg, 0.037 mmol in 2 ml de ethanol-water) were added to a thiosaccharine dissolution (20 mg, 0.1 mmol / 2 ml ethanol-water 1:1). A 2,2'-bipyridine dissolution was then added (5.8 mg, 0.0371 mmol/ 2 ml de ethanol-water). A light yellowish precipitate was formed and filtered. It was washed with

distilled water. By slow diffusion of ethyl ether to a saturated ethanol-water solution very thin needles appeared. Yield: 85%. Molar conductivity (μS M^{-1}) = 18.2. Analytical percent composition calculated for $C_{24}H_{16}N_4O_4S_4Zn$: C=46.642%; H=2.6093%; N=9.0648%. Found: C=46.422%; H=2.335%; N=8.893%.

Soluble in dimethyl sulfoxide and dimethylformamide. Slightly soluble in water, ethanol, methanol, acetone and chloroform. UV-Visible [DMSO, λmax nm]: 343

^{1}H NMR (300 MHz, DMSO) δ 8.60-8.90 (d, 1H), 8.73 (d, 1H), 8.34 (t, 1H), 7.94 (m, 1H), 7.83 (m, 1H), 7.58-7.75 (m, 3H). 13C NMR (75 MHz, DMSO) δ 191.73 (C1), 148.47 (C9), 141.43 (C10), 137.81 (C7), 137.75 (C12), 136.33 (C2), 132.19 (C4), 131.03 (C5), 127.09 (C8), 125.14 (C3), 122.79 (C11), 119.07 (C6).

[Zn(tsac)$_2$(2,2'-bq)] (5)

A $Zn(NO_3)_2 \cdot 6H_2O$ dissolution (10.3 mg, 0.0346 mmol / 2 ml ethanol:water 1:1) was added to another dissolution of thiosaccharine (12.3 mg, 0.062 mmol / 2 ml ethanol:water 1:1). Finally, solid 2,2'-biquinoline was added (9.4 mg, 0.0367 mmol / 2 ml ethanol:water 1:1). A pale yellow powder was then obtained. Yield: 90%. Molar conductivity (μS M^{-1}) = 26.3. Analytical percent composition calculated for $C_{32}H_{20}N_4O_4S_4Zn$: C=53.520%; H=2.807%; N=7.801%. Found: C=53.884%; H=2.761%; N=7.698%.

Soluble in DMSO and DMF. Almost insoluble in water, ethanol, methanol, acetone, dichloromethane and chloroform. [DMSO, λmax nm]: 339

^{1}H NMR (300 MHz, DMSO) δ 8.80 (dd, 1H), 8.58 (dd, 1H), 8.19 (dd, 1H), 8.08 (dd, 1H), 7.89-7.95 (m, 1H), 7.85 (td, 1H), 7.53-7.73 (m, 4H). ^{13}C NMR (75 MHz, DMSO) δ 191.54 (C1), 155.21 (C16), 147.16 (C8), 137.80 (C7), 137.36 (C14), 136.32 (C2), 132.16 (C4), 130.99 (C5), 130.18 (C10), 129.31 (C12), 128.16 (C13), 128.03 (C11), 127.42 (C9), 125.10 (C3), 119.05 (C6), 118.87 (C15).

2.3 X-ray crystallography

Single crystal X-ray diffraction measurements of **(1), (2)** and **(3)** were carried out with Mo Ka radiation using an Xcalibur, Eos, Gemini diffractometer. Absorption was corrected for by multi-scan methods, CrysAlis PRO (Rigaku OD, 2015). H-atom parameters were constrained. Computer programs used: *CrysAlis PRO* (Rigaku OD, 2015) [Diffractometer control and data reduction], *SHELXS97* (Sheldrick, 2008) [Structure resolution], *SHELXL2014*/6 (Sheldrick, 2015) [Model refinement], *XP* in *SHELXTL* (Sheldrick, 2008), *PLATON* (Spek, 2009) [Analysis of the results].

2.4 Cell line culture and proliferation assays

SVEC cell line stably expressing the viral G protein couple receptor was used (vGPCR cells). vGPCR cells injected into immunosuppressed mice promotes tumour formation; thus inducing angiogenic lesions similar to those developed in Kaposi sarcoma [11,12]. These transfected cells were cultured in DMEM 2.5% foetal bovine serum (FBS) and selected with 500 μg/mL G418 (Cellgro, Manassas, VA). For proliferation studies, cells were seeded in 24-well plates at a density of 12,000 cells per well. After overnight growth, cells were treated with each ternary Zn(II) complexes (**1**,**2**,**3, 4** and **5**) or vehicle (DMSO, 0.1%) in triplicate during 48 h. The time was selected based on the duplication cells time for these growth conditions

and is appropriate to visualize an inhibition of the cell proliferation. At the end of the treatment, cells were harvested and counted in a Neubauer chamber; proliferation was quantified as the percentage of living cells [12].

2.5 Theoretical calculations

The theoretical calculations were performed with Gaussian09 [13]. The initial geometry optimization of complex **1** was performed with the semi empirical PM3 method. The geometry thus obtained was used as starting point for the density functional theory (DFT) [14] calculations, that were performed with the B3LYP functional [15], which is known to be an appropriate methodology for the study on metal thiosacharinates complexes with nitrogen donor co-ligands [9]. Zero point energy was computed at the 6-31+G* level for C, H, S, N and O atoms and employing the LANL2DZ effective core potential basis set for Zn. The characterization of the stationary point was done by Hessian matrix calculations of geometries obtained with full optimization for a minimum. The vibrational frequency analysis showed no imaginary frequencies. All calculations were performed in gas phase. The structure figure (see Supp. Info S22) was built with the VMD program.

3. Results and Discussion

3.1 Crystal structures

Table 1 summarizes crystal data, data collection procedures, structure determination methods and refinement results for complexes (**1**), (**2**) and (**3**). Table 2 presents some selected distances and angles, and Table 3 shows the most relevant H-bonding interactions.

Figures 1-3, in turn, show molecular representations of the complexes. Full structural information has been deposited in cif format at the Cambridge Crystallographic Data Centre, under deposition numbers CCDC 1812462 (**1**), CCDC 1812463 (**2**) and CCDC 1812464 **(3).**

Table 1. Crystal and refinement data

	$[Zn(tsac)_2(o\text{-}phen)]$ (**1**)	$[Zn(tsac)_2(TMDP)]n$ (**2**)	$[(4,4'\text{-}bipy)H_2][Zn(tsac)_4]$ (**3**)
Crystal data			
Chemical formula	$C_{26}H_{16}N_4O_4S_4Zn$	$C_{27}H_{22}N_4O_4S_4Zn$	$C_{38}H_{26}N_6O_8S_8Zn$
M_r	642.04	660.09	1016.50
Crystal system, space group	Monoclinic, *I*2/*a*	Monoclinic, $P2_1/c$	Orthorhombic, *Fddd*
Temperature (K)	293	295	293
a, *b*, *c* (Å)	15.0832 (4), 10.4741 (3), 16.6559 (6)	11.8808 (5), 16.0116 (7), 15.4802 (5)	10.2455 (6), 26.4252 (9), 29.2967 (11)

α, β, γ (°)	90, 91.275 (3), 90	90, 96.684 (3), 90	90, 90, 90
V (Å^3)	2630.69 (14)	2924.79 (19)	7931.8 (6)
Z	4	4	8
μ (mm^{-1})	1.29	1.17	1.10
Crystal size (mm)	0.32 × 0.22 × 0.18	0.18 × 0.18 × 0.14	0.28 × 0.20 × 0.16
Data collection			
T_{min}, T_{max}	0.72, 0.78	0.73, 0.81	0.72, 0.86
No. of measured, independent and observed [I > 2s(I)] reflections	5737, 2851, 2213	25094, 6761, 4812	14567, 2430, 1932
R_{int}	0.021	0.066	0.036
(sin θ/λ)$_{max}$ (Å^{-1})	0.675	0.670	0.685
Refinement			
R[F^2 > 2σ(F^2)], ωR(F^2), S	0.034, 0.090, 1.01	0.068, 0.210, 1.01	0.035, 0.091, 0.98
No. of reflections	2851	6761	2430
No. of parameters	177	361	140
Δρ$_{max}$, Δρ$_{min}$ (e Å^{-3})	0.27, -0.34	1.34, -0.82	0.37, -0.26

Table 2

Selected bond distances and angles [Å,°]

(1)				
	Zn1—N1B	2.0723 (19)	S2A—C7A	1.698 (2)
	Zn1—N1B (calculated)	2.144	S2A—C7A (calculated)	1.735
	Zn1—S2A	2.2952 (7)	N1A—C7A	1.308 (3)
	Zn1—S2A (calculated)	2.415	N1A—C7A (calculated)	1.306
	N1B—Zn1—N1B^i	80.81 (11)	N1B—Zn1—S2A^i	110.50 (5)
	N1B—Zn1—N1B^i (calculated)	117.1	N1B—Zn1—S2A^i (calculated)	
	N1B—Zn1—S2A	120.16 (5)	S2A—Zn1—S2A^i	111.91 (4)
	N1B—Zn1—S2A		S2A—Zn1—S2A^i	107.2

	(calculated)		(calculated)	
Symmetry code: (i) -*x*+1/2, *y*, -*z*+1.				
(2)				
	Zn1—N2C^{i}	2.030 (3)	S2A—C7A	1.701 (4)
	Zn1—N1C	2.049 (3)	N1A—C7A	1.310 (5)
	Zn1—S2A	2.3085 (14)	S2B—C7B	1.703 (4)
	Zn1—S2B	2.3220 (12)	N1B—C7B	1.312 (5)
	N2C^{i}—Zn1—N1C	107.60 (13)	N2C^{i}—Zn1—S2B	108.39 (10)
	N2C^{i}—Zn1—S2A	109.38 (10)	N1C—Zn1—S2B	104.34 (9)
	N1C—Zn1—S2A	109.52 (10)	S2A—Zn1—S2B	117.15 (5)
Symmetry code: (i) *x*+1, *y*, *z*.				
(3)				
	Zn1—S2	2.3598 (6)	N1—C7	1.311 (3)
	S2—C7	1.695 (2)		
	S2—Zn1—S2^{i}	96.75 (3)	S2—Zn1—S2^{iii}	123.25 (3)
	S2—Zn1—S2^{ii}	109.53 (3)		
Symmetry codes: (i) -*x*+1/4, -*y*+1/4, *z*; (ii) *x*, -*y*+1/4, -*z*+1/4; (iii) -*x*+1/4, *y*, -*z*+1/4.				

Table 3

Hydrogen-bond geometry (Å, º)

	D—H···*A*	*D*—H	H···*A*	*D*···*A*	*D*—H···*A*
(1)					
	C2*A*—H2*AA*···O1*A*^{ii}	0.93	2.36	3.072 (3)	134
	C2*B*—H2*BA*···S2*A*^{iii}	0.93	2.74	3.538 (3)	144
Symmetry codes: (ii) -*x*, *y*-1/2, -*z*+1/2; (iii) *x*-1/2, -*y*+1, *z*.					
(2)					
	C2B—H2B···O2Ai^{i}	0.93	2.44	3.330 (6)	159
	C10C—H10C···S2A^{iii}	0.93	2.95	3.777 (4)	149
Symmetry codes: (ii) *x*+1, -*y*+1/2, *z*+1/2; (iii) -*x*, *y*-1/2, -*z*+1/2.					

(3)					
	N11—H11N···O1^{iv}	0.86	2.47	3.134 (3)	134
	C11—H11···O2^{iv}	0.93	2.35	3.137 (3)	142
	C21—H21···O2^{v}	0.93	2.47	3.149 (3)	130
	C6—H6···O1^{vi}	0.93	2.55	3.400 (3)	152
Symmetry codes: (iv) *x*+1/4, -*y*+1/2, *z*-1/4; (v) -*x*+5/4, *y*, -*z*+1/4; (vi) -*x*+3/4, -*y*+3/4, *z*.					

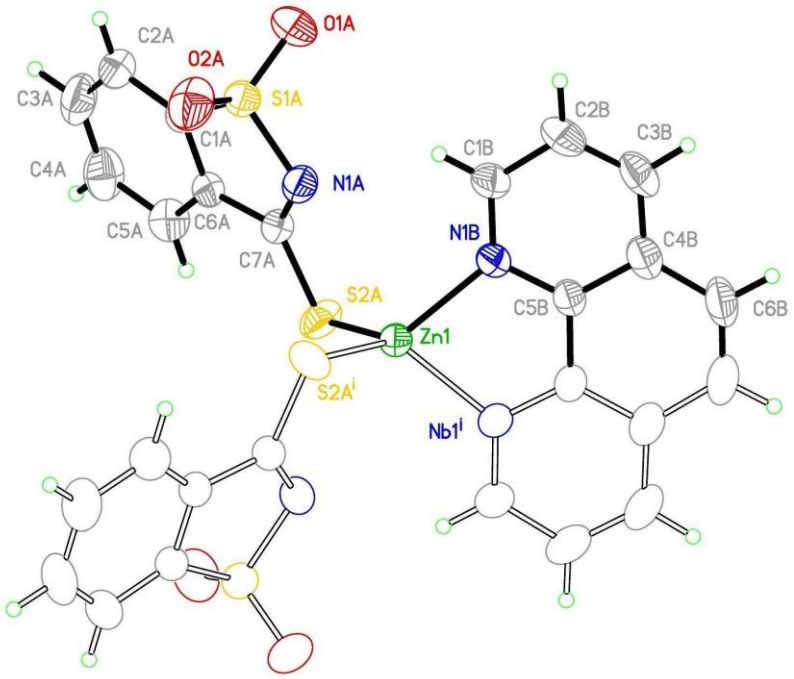

Figure 1: Molecular representation of [Zn(tsac)$_2$(o-phen)] (**1**)
Symmetry code: (i) -*x*+1/2, *y*, -*z*+1.

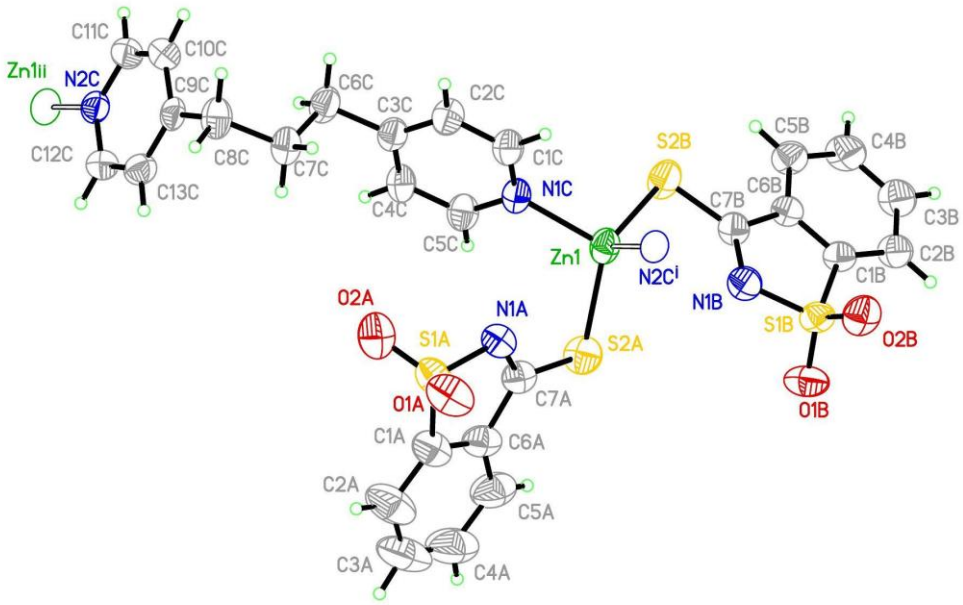

Figure 2. Molecular representation of $[Zn(tsac)_2(TMDP)]_n$ (**2**)
Symmetry code: (i) *x*+1, *y*, *z*.

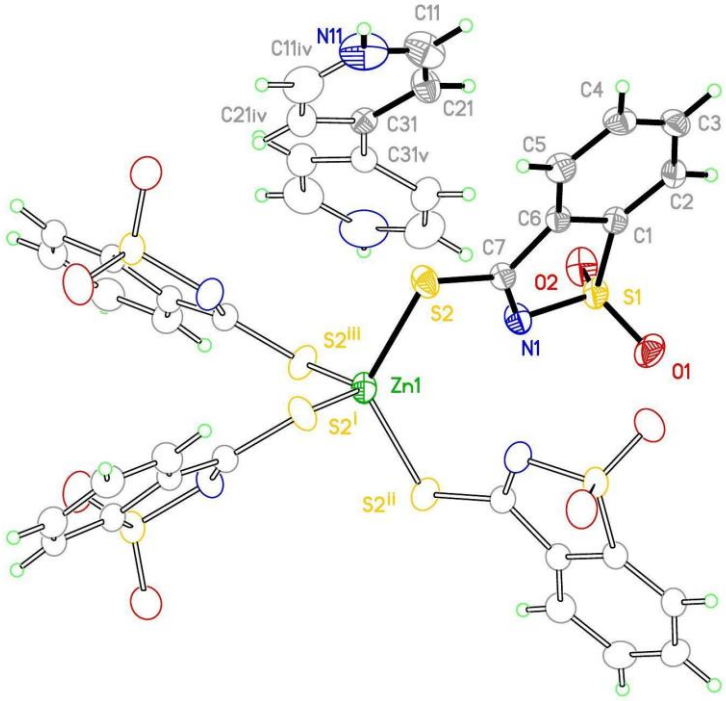

Figure 3. Molecular representation of $[(4,4'\text{-bipy})H_2][Zn(tsac)_4]$ (**3**)

Symmetry codes: (i) -*x*+1/4, -*y*+1/4, *z*; (ii) -*x*+1/4, *y*, -*z*+1/4, (iii) *x*, -*y*+1/4, -*z*+1/4.

[Zn(tsac)$_2$(o-phen)] (1)

The solid state structure of complex [Zn(tsac)$_2$(o-phen)] consists in discrete molecular species, bisected by a twofold rotation axis, with the Zn atom being located in the center of a distorted tetrahedron, surrounded by two thiosaccharinate anions and by a molecule of ortho-phenanthroline. The two thiosaccarinate anions monocoordinate through the exocyclic sulfur atom to the metal center. The o-phenanthroline molecule quelates the metal atom through both pyridinic N atoms. Bond distances around the Zn atom can be seen in Table 2. Figure 1 is a molecular representation of the complex. The phenantroline molecule and the two anions presented almost planar structures, as expected. A comparison of the metal–ligand bond distances in complex (**1**) with the distances in other mixed ligand Zn thionates with ortho-phenantroline, show that they are average Zn-S (Zn-S_{tsac} 2.2952 (7) Å) and Zn-N (Zn-N_{phen} 2.0723 (19) Å) bond distances for this type of complexes [16, 17]. The tetrahedral deviation is evidenced by the deviation of the bond angles from the ideal angle of a tetrahedral geometry (109.5°): N1B—Zn1—S2A^i (110.50 (5)), N1B—Zn1—N1B^i (80.81 (11)), N1B—Zn1—S2A (120.16 (5)) and S2A—Zn1—S2A^i angles (111.91 (4)). This deviation is attributed to the steric demand of the chelating di-pyridinic ligands. The Zn-N_{py} is within the range reported by García Vazquez for similar complexes with pyridine-2-thione.

[Zn(tsac)$_2$(TMDP)]$_n$ (2)

In the [Zn(tsac)$_2$(TMDP)]$_n$ complex the metal center adopts a slightly distorted tetrahedral geometry (angles around the metal center 110.5, 117.7, 107.8 and 105.9º). The anion is monocoordinated through the exocyclic S atom. The trimetilenedipyridine molecule coordinates through the nitrogen atoms, bridging two metal centers. In this complex, [Zn(tsac)$_2$(TMDP)], the Zn-S bond distances (Zn-S(1) 2.326 Å y Zn-S(2) 2.302 Å) are longer than the bond distances in [Zn(tsac)$_2$(o-phen)] (2.296 Å) but shorter than the distances presented by [(4,4'-bipy)H$_2$][Zn(tsac)$_4$] (2.357 Å). Regarding the Zn-N_{py} bond distances (Zn-N(1) 2.071 Å and Zn-N(2) 2.049 Å) they are within the range reported by Zheng et al. for other Zn complexes coordinated with similar nitrogenated ancillary ligands [18].

[(4,4'-bipy)H$_2$]$^{2+}$[Zn(tsac)$_4$]$^{2-}$] (3)

Among the different zinc complexes reported in the literature, 4,4 -bipyridine has been used as a two connector in many studies to construct transition metal networks having a wide variety of structures. The thiosaccharinate complex shows an ionic structure, with the metal center located at a highly symmetric site (the intersection of three orthogonal two fold axis). This Zn atom is located in a tetrahedral geometry, surrounded by four symmetry related thiosaccharinate anions, builds up the anion. The four thionates are coordinated to the metal through the sulfur atom. Each of the four anions presents a cuasi planar structure. The structure of the complex is completed by a di-protonated 4,4'-bipyridine molecule, acting as counter anion. In the literature, 4,4'-bipyridine is reported in several Zn compounds as a neutral connector, building polymeric complexes (as reviewed by A. Erxleben [19]). However, there are also reports of different compounds with the nitrogenated ligand acting mono-protonated, [(4,4'-bipy)H]$^+$ [20] and di-protonated, [(4,4'-bipy)H$_2$]$^{2+}$ [21]. The bond distance between the thiocarbonilic S and the Zn metal atom is longer than the same distance in the complexes (**1**) and (**2**), where the Zn atoms

are surrounded by only two thiosaccharinates (2.357 Å in (**3**) *vs* 2.296 Å in (**1**) or 2.326/2.302 Å in (**2**)).

The analysis and comparison of the thiocarbonilic moieties within the three different Zn thiosacharinates show that this group suffers different modifications after the coordination. These changes are not only related to the coordinated atoms but also to the pka of the di-pyridines. Whereas complexes **(1)** and **(2)** have the same coordination sphere, ZnS_2N_2, complex (**3**) has a different structure, surrounded by four sulfur atoms, ZnS_4. The thiocarbonilic S-C distance varies from (1.698 Å complex **(1)** to 1.684 Å in (**3**) and a very similar value for complex **(2)** S-C bond distance, 1.685 Å). Linked to this value, the C-N bond distances is shortened for complex **(1)** (1.305 Å),but enlarged in complex **(2**) and **(3)** respectively (1.305 Å and 1.312 Å). The C1–S1 bond distance in the "free" thiosaccharinate anion, reported in 2006 [23 d], (1.678(2) Å) is shorter than the three C-S thiocarbonilic bond distances observed for the Zn thiosacharinates, confirming the coordination. The N-C thiocarbonilic bond distance for the free anion, (1.324 Å) is in the middle of the range of the values observed for the Zn thiosacharinates.

In all three compounds **(1), (2)** and **(3),** the H-bonding schemes (summarized in Table 3) lead to weakly connected 3D structures.

Ali *et al* summarized the molar conductance ranges of metal complexes in different solvents [22]. The values measured for our Zn complexes, as expected, are in agreement with the crystal structures found. Ali stated that the molar conductance for non-electrolytic complexes, in DMSO, should be <50µS M^{-1}. The values found for **(1)**, **(2)**, **(3)** and **(4)** are respectively 22.4, 28.3, 18.2 and 26.3 µS M^{-1}, which supports non-electrolytic behavior in solution. For complex **(3),** the molar conductivity of 138.7 µS M^{-1} clearly indicates an electrolytic behavior. The range reported for 1:1 electrolyte, 50-90 µS M^{-1}, is lower than the value found for **(3)**. This is due to the fact that complex **(3)** $[(4,4'\text{-bipiyH}_2][Zn(tsac)_4]$ is a 1:1, anion:cation, electrolyte with $[(4,4'\text{-bipiyH}_2]^{++}$ and $][Zn(tsac)_4]^{=}$.

3.2. Vibrational and electronic spectra

The five complexes were characterized by FTIR spectroscopy. All the bands due to the ligands are present in the spectra. A selection of the thiosaccharinate characteristic bands and some of the co-ligands and their assignments are presented in Table 4. The assignments have been made considering the theoretical calculations performed for complex previous published theoretical vibration analysis [23] and based on our previous studies on metallic and ionic thiosaccharinates [9 and references therein]. The vibrational spectra of complexes (**1**), (**2**) and (**3**) are consistent with their X-ray structure. The most interesting bands of these compounds are those related to the five-member ring of the thiosaccharinate anions, located between 1500 and 400 cm^{-1}. The thione benzene ring vibrations show no significant differences compared with the thione benzenic ring vibrations of Htsac or PNP(tsac) (bis(triphenylphosphine)-iminium thiosaccharinate) [24]. The bands attributable to the N-H bond vibrations, namely ν(NH) and δ(NH) modes, which in the thiosaccharine molecule appear at 3341 and 1376 cm^{-1}, respectively, are absent in the spectra of the five new complexes. The ν(SH) absorption region is also free of bands (between 3000 and 2550 cm^{-1}). The stretching motion of the reinforced C-N bonds bands appear in all the complexes at higher wavenumbers compared to the values found for the thiosaccharinate in PNPtsac (in which the thiosaccharinate is considered as a free anion). Those bands due to the weakened stretching of the C-S bonds shift (1003, 1006, 1002 and 977 cm^{-1}) to lower frequencies (for PNP(tsac) ν(CN):1365, and $\nu(CS_{exo})$:1010 cm^{-1}). These frequency

movements reproduce the changes in the strength of the bonds within the thioamidate groups after the coordination. Complex (**3**) spectrum shows the 4,4'-bipyridine's N-H stretching band at 3080 cm^{-1}, in accordance with the reported values for the protonated bipyridine [25]. It is interesting to note that for complexes (**4**) and (**5**), which could not be crystallized, the bands assigned to the $\nu(CS_{exo})$ are red shifted for both complexes if compared to the other three. This fact may be indicating that the anions in these complexes are coordinating in a different mode, with a weakened CS_{exo} bond. Therefore, we postulate that the thiosaccharinate anion in this complexes are bridging two metal centers with long Zn-S bonds, as in complex $[Ag(tsac)(o\text{-}phen)]_n$ [26] and consequently weakening the S_{exo}-C bond, which in turn is reflected in the shift of the $\nu(C\text{-}S_{exo})$. Thus, based on the elemental analysis and on the FTIR spectra, we propose that complexes (**4**) and (**5**) could be formed by polymeric structures, in which the S atoms bridged two different Zn atoms, and the nitrogenated coligands quelate to the metal center, as expected.

Table 4. FTIR selected vibration frequencies (cm^{-1}) and mode assignments of complexes **1-5**

Assignations	**1** Experimental	**1** Calc.(intensity)	**2**	**3**	**4**	**5**
ν_{σ}(CN)pi	1601m	1529 (289)	1619m	1600m	1598m	1593m
ν(CN)δ(ϕS)	1423s		1431s	1405s	1441m	1470m
νas(SO_2)	1306vs	1326 (170)	1306vs	1273vs	1310vs	1325vs
δ(CH) ν(CC)	1242m	1249 (406)	1234m	1226vs	1230m	1234m
νs(SO_2) ν(CC)	1161vs	1158 (177)	1158vs	1150vs	1157vs	1164vs
ν(CS) δ(CNS)	1006m	1007 (248)	1003m	1002m	997m	997m
ν(NS) δ(CCC)	805vs		802vs	819vs	808vs	825vs
γ(CH)pi	772vs	772 (224)	768vs	768vs	771vs	790vs
γ(SO_2)	592vs		587vs	593vs	587vs	587vs
δ(SO_2) δ(CS)	558m		555m	552m	553m	553m
δ_{ϖ}(SO_2)	522m		534m	535vw	541m	539m
γ(CCC)pi	429vw		430vw	432m	431m	431m

ν: stretching, δ: in plane bending, γ: out of plane bending, ϕ: bencenic ring, as: asymmetric, s: symmetric, iso: isoindolic ring, vs: very strong, s: strong, m: medium, w: weak. Normal modes wavenumbers calculated with Gaussian

In the electronic spectra of the five complexes recorded in DMSO solutions, only bands due to the $\pi \rightarrow \pi^*$ transitions of the $C–S_{exocyclic}$ group were observed. The rest of the expected bands (e.g. the bands due to the $\pi \rightarrow \pi^*$ transitions of the phenyl rings of the anion or of the other ligands) where overlapped by the absorption bands of the DMSO solvent.

3.3. ^{1}H and ^{13}C NMR spectral studies

The NMR spectra of the new complexes, in DMSO-d^6 solutions, were studied and compared to the NMR responses of other metal thiosaccharinates with nitrogenated ligands. The numbering scheme of the anions are shown in Scheme 1.

Scheme 1. Atoms numbering for the NMR signals assignments

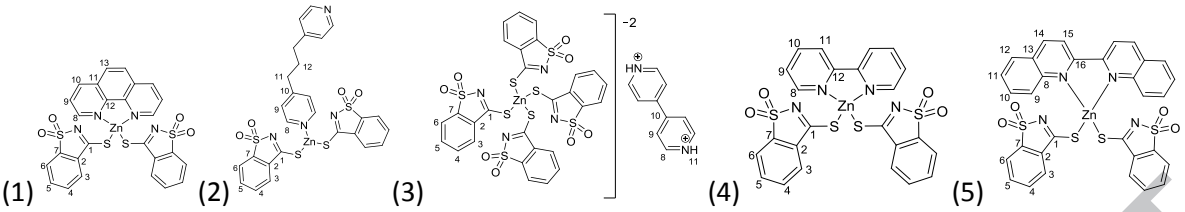

In the ^{1}H-NMR spectra of [Zn(tsac)$_2$(o-phen)], complex (**1**), the characteristic signals of orto-phenantroline appear at 9.18 (d, 1H, H8), 8.93 (d, 1H, H10), 8.31 ppm (m, 1H, H13) and the other proton (H9) appears between 8.03-8.21 ppm. These values are shifted if compared with those reported by Pazderski et al) [27] (9.11 and 7.79 ppm respectively). Regarding the thiosaccharinate protons the characteristic signals appear at 7.57-7.72 (m, 3H, H4/H5/H6) and 7.91 (m, 1H, H3) ppm. Those are values well in the range of other metal thiosaccharinates previously reported [9]. For complex (**2**), [Zn(tsac)$_2$(TMDP)], the TMDP proton signals appear at 8.46 ppm (dd, 4H, H8), 7.28 ppm (dd, 4H, H9), 2.64 ppm (t, 4H, H11) and 1.93 ppm (m, 2H, H12). The thiosaccharinate anions show their proton resonances at 7.92 ppm (m, 2H, H3) and 7.58-7.72 ppm (m, 6H, H4/H5/H6). The ^{1}H-NMR spectra of complex (**3**), [(4,4'-bipy)H$_2$][Zn(tsac)$_4$], show the characteristic signals of the 4,4'-bipy: 8.98 ppm (dd, 4H, H8) and 8.30 ppm (dd, 4H, H9). The thiosaccharinate protons appear at 7.87-7.08 ppm (m, 4H, H3), 7.73-7.81 ppm (m, 4H, H6) and 7.35-7.72 (m, 10H, H4/H5/H11). Complex (**4**) NMR spectra, shows the 2,2'-bipyridine signals at 8.60-8.90 (m, 1H, H9), 8.73 (d, 1H, H11), 8.34 (t, 1H, H10), 7.83 (m, 1H, H8). For the thiosaccharinate anions, the characteristic signals appear at 7.94 (m, 1H, H3) and 7.58-7.75 (m, 3H, H4/H5/H6). These signals are shifted if compared with the values obtained for [Ag$_2$(tsac)$_2$(2,2'-bipy)$_2$], reported in 2007 by Dennehy *et al*. The 2,2'-bipy appear for that compound at 7.59, 7.98 (dt,4H), 8.20 (dd,4H) and 8.80 (dd,4H) ppm and the thiosaccharinate bands are observed at 7.78 (m,1H), 7.90 (d,1H) and 8.11 (d,1H) [28]. In the ^{1}H NMR spectra of [Zn(tsac)$_2$(2,2'-bq)]$_n$ (**5**), the 2.2'-bq signals appear at 8.80 ppm (dd, 1H, H15), 8.58 ppm (dd, 1H, H14), 8.19 ppm (dd, 1H, H12), 8.08 ppm (dd, 1H, H11), 7.85 (td, 1H, H10) and 7.53-7.73 (m, 1H, H9). The signals due to the thiosaccharinate protons appear at 7.89-7.95 ppm (m, 1H, H3) and 7.53-7.73 ppm (m, 3H, H4/H5/H6). The ^{13}C NMR spectrum of all complexes show the expected chemical shifts of the coordinated thioamidic C1 atom around 190 ppm (C1 (**1**): 191.81(**2**): 191.71 (**3**): 191.56 (**4**):191.73 (**5**):191.54 ppm). Besides, in order to assign completely and correctly all the signals of ^{1}H and ^{13}C for each structure, we registered the 2D-HSQC RMN spectra for the complexes (See Supplementary Information I).

3.4 Theoretical calculations

DFT methods were applied to establish the correlation between the physical parameters found experimentally for the complex 1 and those calculated. The gas phase geometric structure of this complex was optimized and the vibrational spectrum was predicted. The distances obtained are a good reproduction of the experimentally observed structural parameters. The observed differences are in the range of those previously reported for other silver thiosaccharinates [9]. The differences among calculated and experimental angles are due to the packing in the solid state. The nature of the vibration modes corresponding to complex were in good agreement with the calculated (see Tables 2 and 4).

3.5 Proliferation assays

It was mentioned in the introduction that several Zinc based compounds have antifungal and antibacterial uses. This prompted us to test whether the complexes synthetized here have anti-proliferative actions in endothelial tumor cells. We used endothelial cells transformed by the

viral G protein coupled receptor (vGPCR) of Kaposi's Sarcoma-Associated Herpesvirus, a key molecule to develop Kaposi's sarcoma disease. Thus, cells were treated with each ternary Zn(II) complexes (**1**,**2**,**3**,**4** and **5**) or vehicle (DMSO, 0.1%) at different final concentrations during 48 hours (Figure 4 a-c). Then, proliferation was measured as was described in methods' section and results were expressed as percentage of cell number of each complex versus molar concentration. As is observed in Figure 4 A, .Complex (**1)** seems to have more anti-proliferative activity. Gao *et al.* [29] recently reported the use of two Zn complexes with two chelating agents, 1,10'-phenantroline and 2,2'-bipyridine and found that both complexes exhibited important cancer cell inhibitory rate but lower cytotoxicity toward the normal cell lines. Compound **(2)** has a polymeric structure in a solid state, within the cell environment this structural may disrupt into solvated molecular units resulting in terminal mono coordinated TMDP thus decreasing its biological activity in a dose independent fashion. Complex **(3)** being an ionic compound showed as expected low response independent on doses probably to different response towards membrane crossing. Complexes **(4)** and **(5)** have mononuclear structure with the bipyridine moiety quelating the metal center resulting in a slight biological effect. These results gives rise to new questions to be explored regarding the significance of the differences found in the cell response upon either compound and are beyond the scope of this work.

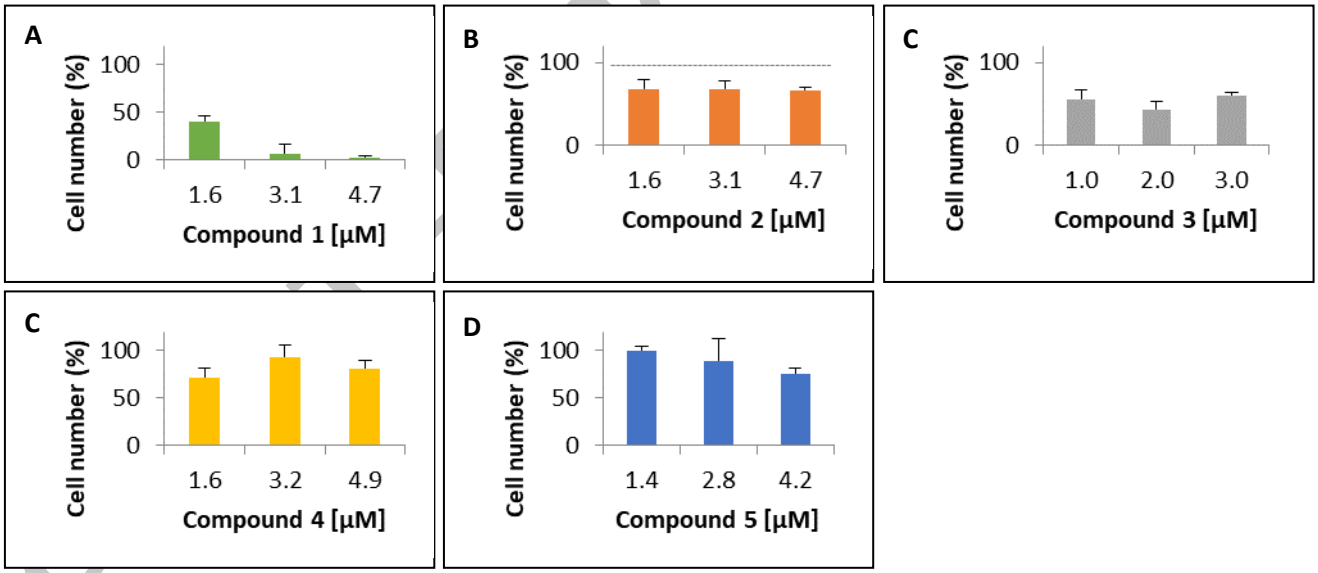

Figure 4. Ternary Zn(II) complexes decrease endothelial vGPCR cells number. Cells were treated with of each complex at different doses: A) compound 1 (1.6-4.7 µM), B) 2 compound (1.6-4.7 µM), C) 3(1-3 µM), D) compound 4 (1.6-4.9 µM), E) compound 5 (1.4-4.2 µM) or vehicle (DMSO) in DMEM 2% FBS for 48 h. Cells were then harvested and counted in a Neubauer chamber. Proliferation was calculated as percentage of leaving cells in treated conditions versus vehicle (dash line) Percentage values (mean ± S.D.) were then represented in bar graphs. n=3.

4. Conclusions

Five new ternary Zn(II) complexes were synthesized and characterized. The metal atoms in all the complexes are coordinated by thiosaccharinate anions and by other nitrogenated ligands. For

three of them, $[Zn(tsac)_2(o\text{-phen})]$, $[Zn(tsac)_2(TMDP)]_n$ and $[(4,4'\text{-bipy})H_2][Zn(tsac)_4]$, the crystal structures showed the expected tetrahedral typical structure for Zn(II) thionates. The anios are coordinated by the exocyclic sulfur atom, not showing coordination through the N thioamidic atom. The proposed structure for the other two complexes consists in a polymeric chain formed by thiosaccharinate sulfur bridges. The coordination of the anion was also confirmed by means of FTIR and NMR studies. Promising results suggested an anti-cancer activity of these ternary Zn(II) complexes.

5. Acknowledgements

M.D. and F.D. gratefully acknowledge the support of this project (Project M24/Q075) by SGCyT-UNS. E.F., V.D. and V.G.P. are researchers from CONICET (Consejo Nacional de Investigaciones Científicas y Técnicas).

6. Supplementary material

Crystallographic data for these structures have been deposited with the Cambridge Crystallographic Data Centre as supplementary data Nros CCDC 1812462, CCDC 1812463 and CCDC 1812464 for $[Zn(tsac)_2(o\text{-phen})]$, $[Zn(tsac)_2(TMDP)]_n$, and $[(4,4'\text{-bipy})H_2][Zn(tsac)_4]$, respectively. Copies of the data can be obtained free of charge upon request from The Director, Cambridge Crystallographic Data Centre, 12 Union Road, Cambridge CB2 1EZ, UK. (fax: +44 1233 336033; e-mail: deposit@ccdc.cam.ac.uk; WEB: http://www.csdc.cam.ac.uk). Additional information regarding ^{1}H and ^{13}C and HSQC NMR spectra for complexes. *xyz* coordinates, calculated frequencies and total energy in atomic units for $[Zn(tsac)_2(o\text{-phen})]$ are available as supplementary information.

7. References

[1] S. Frassinetti, G. Bronzetti, L. Caltavuturo, M. Cini, C.D. Croce. The role of zinc in life: a review. J. Environ Pathol Toxicol Oncol., 25(2006) 597-610.

[2] A. Krężel and W. Maret. The biological inorganic chemistry of zinc ions. Archives of Biochemistry and Biophysics, 611 (2016) 3-19.

[3] A. A. Abdel Aziz, F. M. Elantabli, H. Moustafa, S. M. El-Medani, Spectroscopic, DNA binding ability, biological activity, DFT calculations and non linear optical properties (NLO) of novel Co(II), Cu(II), Zn(II), Cd(II) and Hg(II) complexes with ONS Schiff base, J. of Mol. Structure, 1141 (2017)563-576.

[4] a) S. Mathan Kumar, M.P. Kesavan, G.G. Vinoth Kumar, M. Sankarganesh, G. Chakkaravarthi, G. Rajagopal, et al. New heteroleptic Zn(II) complexes of thiosemicarbazone and diimine Co-Ligands: Structural analysis and their biological impacts. J Mol Struct. 1153 (2018) 1-11.

b) G. V. Scăeţeanu , M. C. Chifiriuc, C. Bleotu,C. Kamerzan, L. Măruţescu,C. G. Daniliuc, C. Maxim, L. Calu,R. Olar, and M. Badea. Synthesis, Structural Characterization, Antimicrobial Activity, and In Vitro Biocompatibility of New Unsaturated Carboxylate Complexes with 2,2′-Bipyridine. Molecules 23(1 (2018) 157-175.

[5] A. Sigel, B. P. Operschall, A. Matera-Witkiewicz, J. Świątek-Kozłowska, H. Sigel, Acid–base and metal ion-binding properties of thiopyrimidine derivatives, Coordination Chem. Rev., 327(2016) 200-220.

[6] S. Barreiro, M. L. Durán-Carril, J. Viqueira, A. Sousa-Pedrares, J. A. García-Vázquez, J. Romero, Structural studies and bioactivity of diorganotin(IV) complexes of pyridin-2-thionato derivatives, Journal of Organometallic Chemistry, 791 (2015) 155-162.

[7] K. Bakhtyar Aziz, Muhamad Barbooti, Subhi Al-Jibori,Mohammed H.S. Al-Jibori. Thermal Decomposition Study of Platinum(II) and Palladium(II) Thiosaccharinate Complexes With Supporting Diphosphine or Bipyridine Ligands, J. of Mat. and Env. Sc., 8 (2017) 1365-1374.

[8] S .A. Al-Jibori, M. M.A. Al-Bayati, H. M. Gergees, C. Wagner, G. Hogarth, Cadmium(II) thiosaccharinate (tsac) complexes: Crystal structures of $[Cd(tsac)_2(abtH)_2]$ (abtH = 2-aminobenzothiazole), $[Cd(tsac)_2(bimsH)_2]$ (bimsH = 2-mercaptobenzimidazole) and $[Cd(\mu\text{-}tsac)(tsac)(\kappa^2\text{-}aapH)]_2$ (aapH = 2-acetylaminopyridine), Inorg. Chim. Acta, 459 (2017) 73-79.
[9] R. A. Burrow, G. Z. Belmonte, V. Dorn, M. Dennehy, Three new Ag(I) thiosaccharinate complexes: Synthesis, structural studies, spectral characterization and theoretical analysis, Inorg. Chim. Acta, 450 (2016) 39-49.
[10] S. Schibye, R.S. Pedersen, S.O. Lawesson, Bull. Soc. Chim. Belg. 87 (1978) 229-238.
[11] S. Montaner, A. Sodhi, A. Molinolo, T.H. Bugge, E.T. Sawai, Y. He, Y. Li, P.E. Ray, J.S.Gutkind, Endothelial infection with KSHV genes in vivo reveals that vGPCR initiates Kaposi's sarcomagenesis and can promote the tumorigenic potential of viral latent genes, Cancer Cell 3 (2003) 23–26.
[12] V. González Pardo, D. Martin, J.S. Gutkind, A. Verstuyf, R. Bouillon, A. Russo de Boland, R. Boland, 1alpha,25-dihydroxyvitamin D3 and its TX527 analog inhibit the growth of endothelial cells transformed by Kaposi sarcoma-associated herpes virus G protein-coupled receptor in vitro and in vivo, Endocrinology 151 (2010) 23–31.
[13] Gaussian 09, Revision C.01, M. J. Frisch, G. W. Trucks, H. B. Schlegel, G. E. Scuseria, M. A. Robb, J. R. Cheeseman, G. Scalmani, V. Barone, B. Mennucci, G. A. Petersson, H. Nakatsuji, M. Caricato, X. Li, H. P. Hratchian, A. F. Izmaylov, J. Bloino, G. Zheng, J. L. Sonnenberg, M. Hada, M. Ehara, K. Toyota, R. Fukuda, J. Hasegawa, M. Ishida, T. Nakajima, Y. Honda, O. Kitao, H. Nakai, T. Vreven, J. A. Montgomery, Jr., J. E. Peralta, F. Ogliaro, M. Bearpark, J. J. Heyd, E. Brothers, K. N. Kudin, V. N. Staroverov, T. Keith, R. Kobayashi, J. Normand, K. Raghavachari, A. Rendell, J. C. Burant, S. S. Iyengar, J. Tomasi, M. Cossi, N. Rega, J. M. Millam, M. Klene, J. E. Knox, J. B. Cross, V. Bakken, C. Adamo, J. Jaramillo, R. Gomperts, R. E. Stratmann, O. Yazyev, A. J. Austin, R. Cammi, C. Pomelli, J. W. Ochterski, R. L. Martin, K. Morokuma, V. G. Zakrzewski, G. A. Voth, P. Salvador, J. J. Dannenberg, S. Dapprich, A. D. Daniels, O. Farkas, J. B. Foresman, J. V. Ortiz, J. Cioslowski, and D. J. Fox, Gaussian, Inc., Wallingford CT, 2010.
[14] W. Kohn and I. J. Sham, Phys. Rev., 140 (1965) A1133-1138.
[15] a) C. Lee, W. Yang, W. and R. G. Parr, Phys. Rev. B, 37 (1988) 785-789
b) A. D. Becke, Phys. Rev. A, 38 (1988) 3098-3100,
c) E. Miehlich, A. Savin, H. Stoll and H. Preuss, Chem. Phys. Lett, 157 (1989) 200-206.
[16] A. Rodríguez, A. Sousa-Pedrares, J. A. García-Vázquez, J. Romero and A. Sousa. Electrochemical synthesis and characterization of zinc(II) complexes with pyrimidine-2-thionato ligands and their adducts with N,N donors, Polyhedron, 28 (2009) 2240-2248.
[17] W. Guo, Z. Peng, D. Li and Y. Zhou. Synthesis and structural characterization of zinc(II) and cadmium(II) complexes with 2-oxo-1,3-dithiole-4,5-dithiolate and 1,10-phenanthroline. Polyhedron, 23 (2004) 1701-1707.
[18] Y. Zheng, J. Zhanga and J. Liu. New Zn(II) coordination polymers with 1,3-bis(4-pyridyl)-propane: syntheses, crystal structures and properties. Cryst.Eng.Comm. 12 (2010) 2740-2748.
[19] A. Erxleben. Structures and properties of Zn(II) coordination polymers. Coord. Chem. Rev., 246 (2003) 203-228.
[20] J. Soleimannejad, H. Aghabozorg and S. Hooshmanda. 4-(4-Pyridyl)pyridiniumbis-(pyridine-2,6-dicarboxylato)chromium(III) tetrahydrate. Acta Cryst E. 64 (2008) 564-565.
[21] N. Soltanzadeh and A. Morsali. Syntheses and characterization nano-structured bismuth(III) oxide from a new nano-sized bismuth(III) supramolecular compound. Polyhedron, 28 (2009) 1343-1347.
[22] I. Ali, W. A. Wani and K.r Saleem. Empirical Formulae to Molecular Structures of Metal Complexes by Molar Conductance. Synthesis and Reactivity in Inorganic, Metal-Organic, and Nano-Metal Chemistry, Vol. 43, (2013), 1162-1170.

[23] a) M. Penavić, G. Jovanovski, O. Grupče, Structure of sodium thiosaccharinate monohydrate. Acta Crystallogr C46 (1990) 2341-2344.

b) M. Penavić, O. Grupče, G. Jovanovski, Structure of potassium thiosaccharinate monohydrate Acta Crystallogr. C47 (1991) 1821-1823.

c) O. Grupče, M. Penavić and G. Jovanovski, Structural study of thiosaccharin by single crystal X-ray diffraction and infrared spectroscopy. J. Chem. Crystallog. 24 (1994) 581-586.

d) E.J. Baran, O.E. Piro, J. Zinczuk, Structural and Spectroscopic Characterization of Ammonium Thiosaccharinate Monohydrate Z. Anorg. Allg. Chem. 632 (2006) 437-440.

[24] M. Dennehy, O.V. Quinzani, S.D. Mandolesi, J.A. Güida, G.A. Echeverría, O.E. Piro, Synthesis and spectroscopic characterization of two new thiosaccharinate salts. Molecular structure of bis(triphenylphosphine)iminium thiosaccharinate, PNP(tsac). Monatsch. Chem. 138 (2007) 669–675.

[25] X. Shi, H. Wang, Y. Li, J. Yang, L. Chen, G. Hui, W. Xu and B. Zhao. Spectroscopic Studies on Co(II), Ni(II), Zn(II) Complexes with 4,4`-Bipyridine. Chem. Res. Chinese Universities, 26 (6) (2010) 1011-1015.

[26] M. Dennehy, R. M. Ferullo, O. V. Quinzani, S. D. Mandolesi, N. Castellani, M. Jennings. Unusual coordination in a silver thionate complex. Synthesis, structural characterization and theoretical calculations of dinuclear and polynuclear silver(I) thiosaccharinates with pyridine and 1,10-phenanthroline.Polyhedron, 27 (2008) 2243–2250.

[27] L. Pazderski, J. Tousek, J. Sitkowski, L. Kozerski and E. Szłyk. Experimental and quantum-chemical studies of ^{1}H, ^{13}C and ^{15}N NMR coordination shifts in Pd(II) and Pt(II) chloride complexes with methyl and phenyl derivatives of 2,2'-bipyridine and 1,10-phenanthroline. Magn. Reson. Chem.. 45 (12) (2007) 1045-1058.

[28] M. Dennehy, O. V. Quinzani and M. Jennings. Mono and polynuclear silver(I) complexes with thiosaccharine and triphenylphosphine or 2,2'-bipyridine. Synthesis, spectroscopic and structural characterization. J. of Mol. Struct., 841 (2007) 110-117.

[29] Enjun Gao, Na Sun, Shaozhong Zhang, Yuqing Ding, Xue Qiu, Yang Zhan, Mingchang Zhu, Synthesis, structures, molecular docking, cytotoxicity and bioimaging studies of two novel Zn(II) complexes, European Journal of Medicinal Chemistry, 121 (2016) 1-11

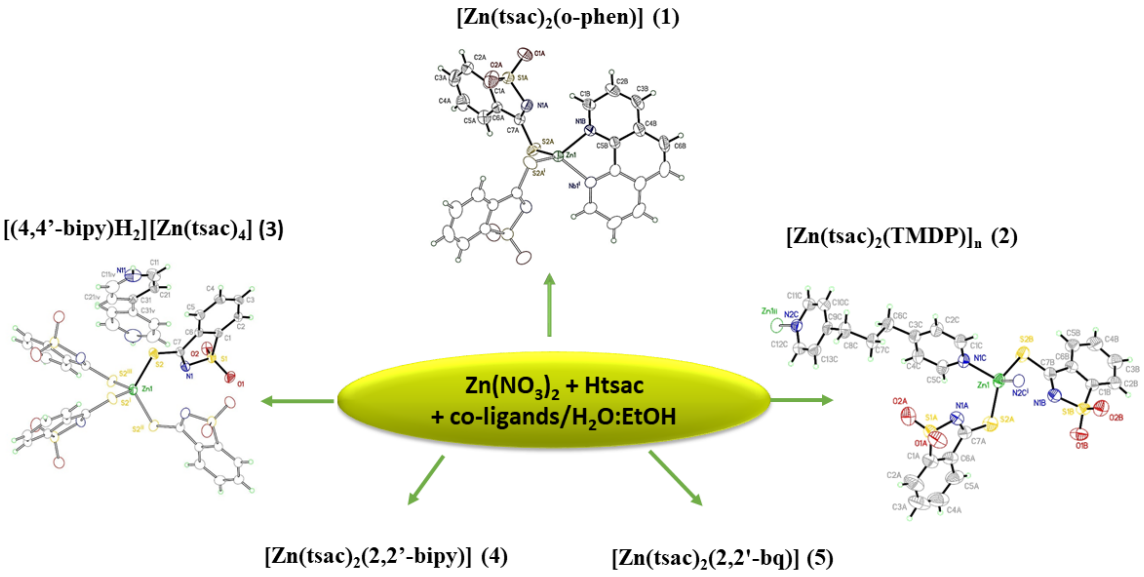

Highlights

- ✓ Five novel Zn thiosaccharinates with N ancilliary ligands are presented in this paper.
- ✓ Three of them ($[Zn(tsac)_2(o\text{-}phen)]$, $[Zn(tsac)_2(TMDP)]_n$, $[(4,4'\text{-}bipy)H_2][Zn(tsac)_4]$) were characterized by X Ray diffraction and their structures are described in the manuscript.
- ✓ Coordination of $[Zn(tsac)_2(2,2'\text{-}bipy)]$ and of $[Zn(tsac)_2(2,2'\text{-}bquin)]$ were inferred from the spectroscopic analysis.
- ✓ The five complexes exhibited anti-proliferative actions in endothelial tumor cells, thus suggesting promising an anti-cancer activity.